

## Crystallization of a polymorphic drug in a stirred tank

C.Herman<sup>a</sup>, V.Gelbgras<sup>a</sup>, V.Halloin<sup>a</sup> and B.Haut<sup>a</sup>

<sup>a</sup> *Chemical engineering department, Université Libre de Bruxelles, Av. Franklin D - Roosevelt, 50  
CP 165/67 B-1050 Brussels, Belgium*

### Abstract

The crystallization process of a drug exhibiting several polymorphic forms is investigated. The study focuses on one reference pharmaceutical crude product. The objective of the work presented in this paper is, on the one hand, to identify the mechanism of the polymorphic transition – from the unstable morph II to the stable morph I –, and, on the other hand, to investigate the influence of the mixing operating conditions on the kinetics of this transition. The study shows that the polymorphic transition follows a mechanism of dissolution (of the morph II) – recrystallization (nucleation and growth of the morph I) mediated by the solvent. Moreover, experimental studies show that the step controlling the beginning of the polymorphic transition is the nucleation of the stable morph I. The mixing plays an important role in this kinetics as the mixing operating conditions influence the metastable zone width.

Keywords: crystallization, polymorphism, modelling, mixing

### 1. Introduction

Crystallization by cooling followed by separation of the crystals from the resulting suspension is the most frequent method to achieve the required purity of active pharmaceutical ingredients (Mersmann A., 1995). However, this method may generate several types of polymorphs (Veesler S. et al., 2003). Hereafter, the crystallization behaviour of a drug exhibiting several polymorphic forms is investigated.

The chosen industrial process consists on the polymorphic crystallization of one reference pharmaceutical crude product. For the purpose of this study, the industrial installation has been reproduced in the lab, on an experimental small-scale pilot installation [*Figure 2*].

As in the industrial process studied, the reference pharmaceutical crude product is initially dissolved in an alcohol at high temperature and stirred in a tank.

Figure 1 (left) presents the typical time evolution of the temperature of the solution during the polymorphic crystallization process in the experimental small-scale pilot installation [Figure 2]. Figure 1 (right) presents the solubility ( $C^*$ ) and metastability ( $C^\circ$ ) curves of the two morphs (enantiotropy polymorphic system), as well as the time evolution of the concentration in the solution during the crystallization process in the experimental small-scale pilot installation [Figure 2]. All these curves have been experimentally obtained, but they are schematically presented for confidentiality purpose.

“Point X” corresponds to the initial state of the system before cooling. The cooling of the solution induces the crystallization of the non-desired crystallographic form (morph II) (“point A”) of the drug. This induces an exothermic peak on the temperature curve, in Figure 1 (left).

In order to obtain the desired crystallographic form (morph I), the temperature is further lowered under  $0^\circ\text{C}$  (“point B”) and the system is kept at this constant maturation temperature. The concentration in the solution is then equal to the saturation concentration relative to the morph II,  $C_{II}^*$ , at the maturation temperature, as it can be seen in Figure 1 (right).

A few hours later, after a so called latency time, the concentration of the solution is still equal to the solubility of the morph II at the maturation temperature (“point C”). Then, at “point C”, the transition from the morph II to the morph I is initiated. This can be observed in Figure 1 (left) by an exothermic peak, and, in Figure 1 (right), by the shift, at the maturation temperature, from the saturation concentration relative to the morph II (“point C”) to the solubility of the morph I,  $C_I^*$  (“point D”).

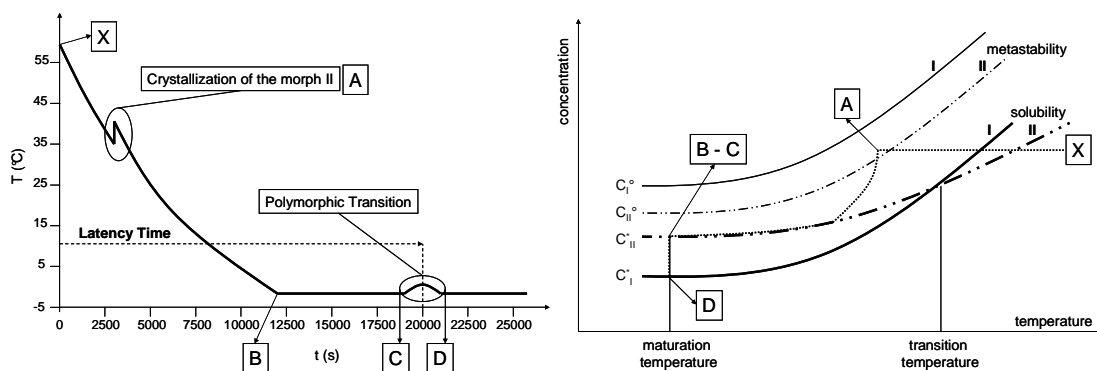


Figure 1: (left) temperature profile during the polymorphic crystallization process as a function of the time - (right) metastability & solubility curves of the two morphs, and time evolution of the concentration in the solution during the polymorphic crystallization process (experimental results on the small-scale pilot installation)

Crystallization of a polymorphic drug in a stirred tank

The objective of this work is, on the one hand, to identify the mechanism of the polymorphic transition at the maturation temperature (shift from the “point C” to the “point D”), and, on the other hand, to investigate the influence of the mixing operating conditions on the latency time.

## 2. Methods and Materials

Batch crystallization experiments are carried out in a double – jacketed glass tank of 1 l, as it can be seen in *Figure 2 (left)*. The initial concentration in the solution containing the reference pharmaceutical crude product is  $0,6 \text{ g}_{\text{product}}/\text{g}_{\text{solution}}$ , and the initial temperature is  $60 \text{ }^{\circ}\text{C}$ .

A mixture (ethanol and water) is thermostated by a thermoelectric Huber PID controller and circulated through the middle jacket to control the speed of cooling, fixed at  $15,5 \text{ }^{\circ}\text{C} / \text{h}$ , and the maturation temperature, set to  $- 2 \text{ }^{\circ}\text{C}$ .

The mixing of the solution is ensured by a stirrer equipped with various impellers types (propeller, Rushton turbine and anchor [*Figure 2 (right)*]) rotating at different speeds, ranging from 100 rpm to 550 rpm.

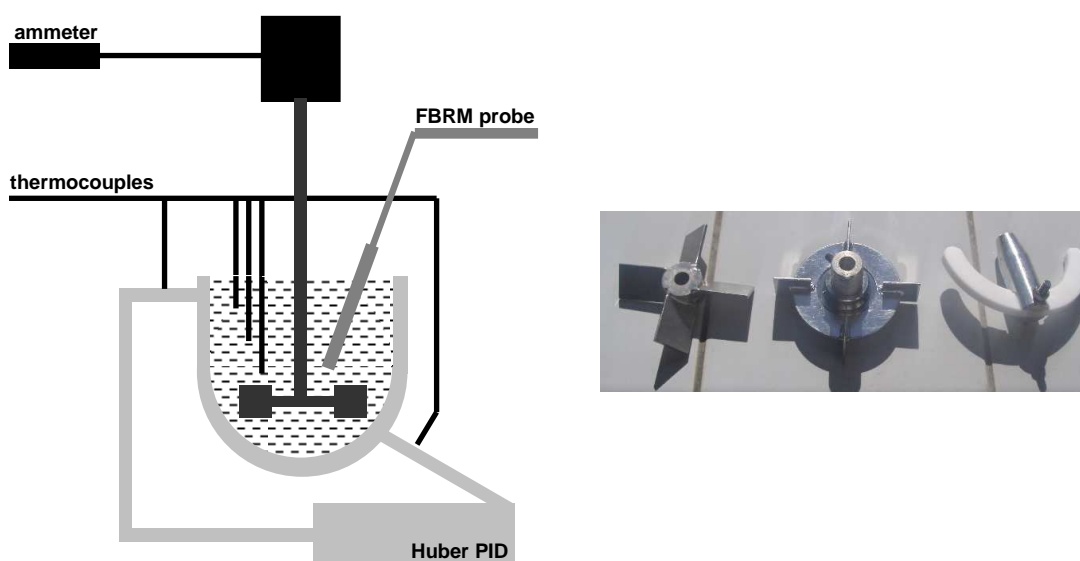


Figure 2: (left) experimental small-scale pilot installation - (right) impellers [left: propeller - middle: Rushton turbine - right: anchor]

Different measurements equipments are used [*Figure 2 (left)*]:

- In – situ Lasentec Focused Beam Reflectance Measure probe: this probe placed within the solution filling the tank is composed of a laser rotating at a fixed speed. The time during which the laser detects a crystal determines a size of chord. The probe continuously measures a Chord Length Distribution, which can be converted into a Crystal Size Distribution by a statistical treatment.

- In – situ type T thermocouples: these thermal probes are placed in various positions within the experimental installation (in the solution in the tank and in the mixture in the middle jacket) to record the time evolution of the temperature during the crystallization process.
- On – line APPA 350 ammeter: this apparatus is used to measure the tension (in Volt) and the current (in A) needed to sustain the rotation of the stirrer at the fixed stirring rate. This can give information about the time evolution of the power dissipated in the suspension held in the tank during the crystallization experiments.

### 3. Results and Analysis

#### 3.1. Mechanism of the polymorphic transition

The mechanism of the polymorphic transition can often be described as a mechanism of « dissolution – recrystallization » mediated by the solvent. (Garcia E. et al., 1999 & 2002 – Veessler. S et al., 2003) As presented in the three following sub-sections, it can be concluded from different experimental results that the polymorphic transition studied in this paper follows such a kind of mechanism.

##### 3.1.1. Optical microscopy

As it can be seen in *Figure 3*, the experimental characterisation of the two morphs by optical microscopy shows that the crystal size of the non-desired morph II is larger than the crystal size of the desired morph I. This observation leads of course to think that the polymorphic transition follows a mechanism of dissolution (morph II) – recrystallization (morph I).

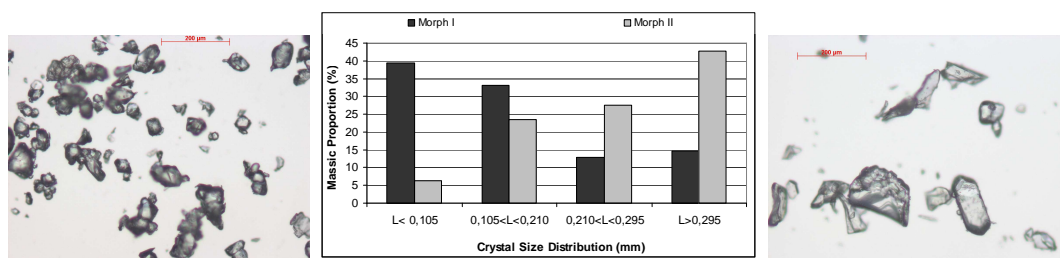


Figure 3: (left) morph I by optical microscopy – (middle) Crystal Size Distribution for the morphs I and II – (right) morph II by optical microscopy

Crystallization of a polymorphic drug in a stirred tank

### 3.1.2. In – situ Focused Beam Reflectance Measure probe

A second way to investigate the mechanism of the polymorphic transition is the analysis of the FBRM probe signal – time evolution of the Chord Length Distribution of the crystals during the crystallization process – as the morphology and the crystal size distribution of the two morphs are quite different [Figure 3]. In Figure 4, the different curves correspond to the time evolution of the number of crystals within a size range.

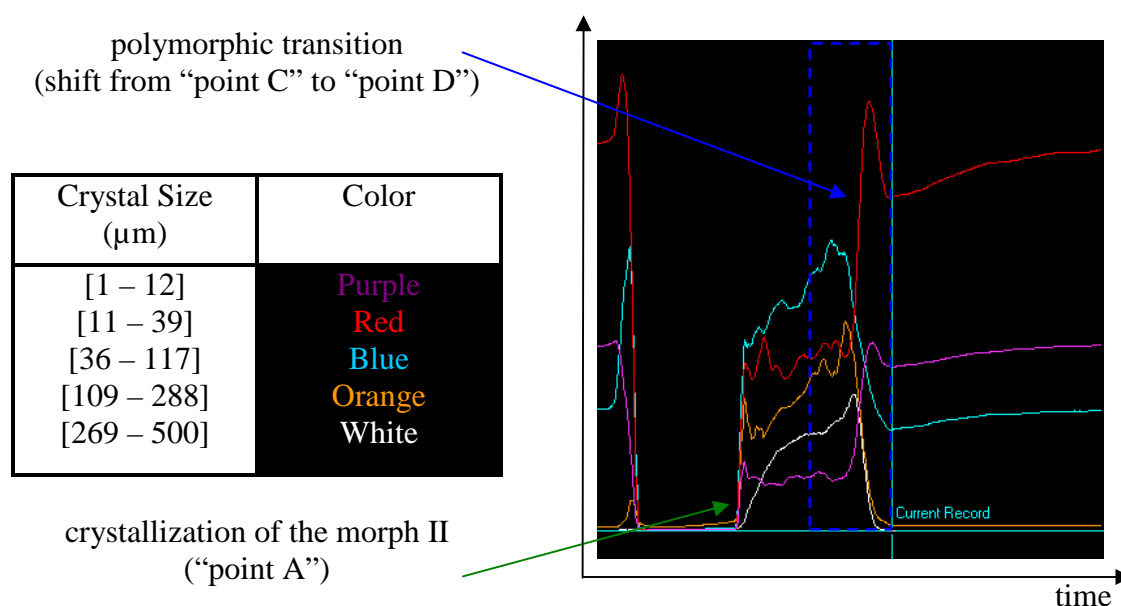


Figure 4: FBRM probe signal during the crystallization process (the different curves correspond to the time evolution of the number of crystals within a size range)

The polymorphic transition takes place in the blue zone. Firstly, the sudden increase of the curves characterising the number of small crystals (purple and red) is observed. It seems to correspond to the nucleation of the morph I crystals. Therefore, it looks like this phenomenon is the step which controls the beginning of the polymorphic transition, and induces large latency times.

Secondly, the sudden decrease of the curves characterising the number of the larger crystals (blue, orange and white) is observed. It seems to result from the dissolution of the morph II crystals. Simultaneously, the growth of the crystals of morph I starts and is carried on.

We can conclude from these experimental results that the polymorphic transition follows a mechanism of dissolution – recrystallization mediated by the solvent.

### 3.1.3. On – line ammeter

A third way to investigate the mechanism of the polymorphic transition is the analysis of the on – line APPA 350 ammeter signal, giving the power needed to sustain the flow in the tank.

An analogy can be done between the power dissipated in the suspension (solution and crystals) and its viscosity.

The time evolution of the temperature and of the power dissipated in the suspension during the polymorphic crystallization process, in the experimental small-scale pilot installation, is shown in *Figure 5 (left)*, while the time evolution of the concentration in the solution during the polymorphic transition at the maturation temperature is schematically represented in *Figure 5 (right)*.

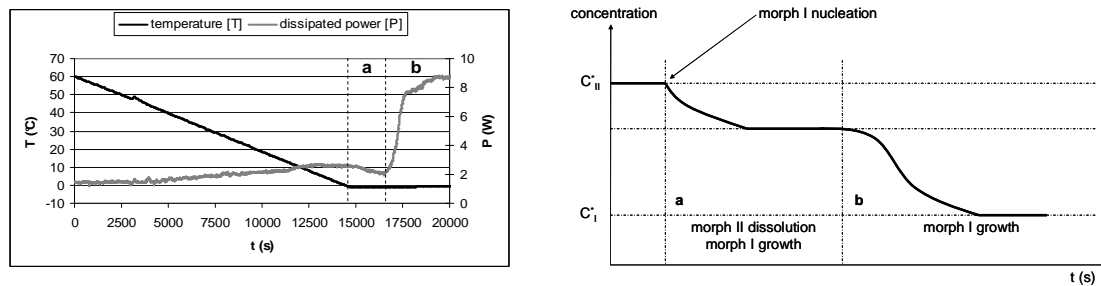


Figure 5: (left) time evolution of the temperature (T) and of the power dissipated in the suspension (P) during the polymorphic crystallization process - (right) time evolution of the concentration in the solution during the polymorphic transition at the maturation temperature

During cooling, the power dissipated in the suspension increases continuously but slowly, due to the increase of the viscosity resulting from the lower temperature as well as from the higher crystal fraction [*Figure 5 (left)*].

A decrease of the power dissipated in the suspension is then observed (phase a). It can be attributed to a lower concentration in the solution due to the simultaneous phenomena of morph II dissolution and morph I nucleation or growth [*Figure 5*].

The next increase of the power dissipated in the suspension results from the growth of morph I which induces an increase of the solid crystals fraction (phase b).

It is interesting to note that the apparent viscosity of the suspension of morph II crystals is lower than the one containing morph I crystals [*Figure 5 (left)*]. This might be linked to the fact that the morph I crystals are much smaller (and hence much abundant) than morph II crystals [*Figure 3*].

### 3.2. Influence of the mixing operating conditions on the latency time

Figure 6 presents experimental results of latency times obtained by varying the mixing operating conditions: the impeller type (propeller, Rushton turbine and anchor [Figure 5 (right)]) and the stirring rate (from 100 rpm to 550 rpm).

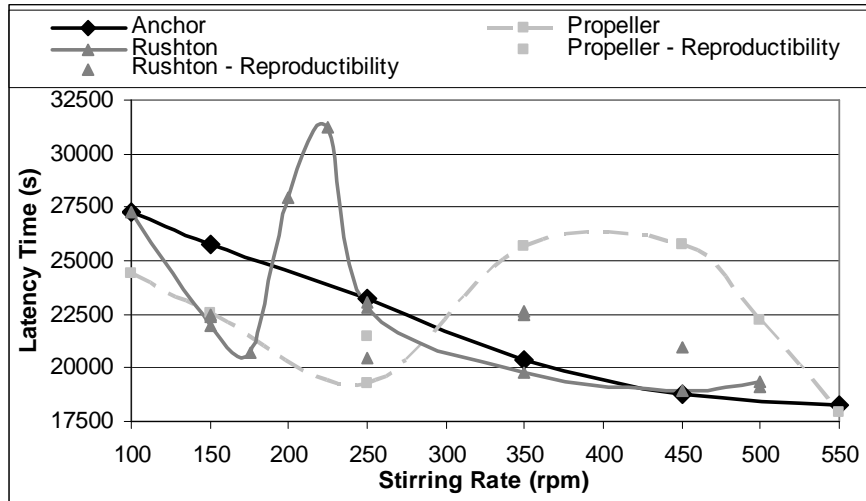


Figure 6: experimental profile of the latency times as a function of the mixing operating conditions

It is quite interesting to note that an analogy can be done between the experimental profile of the latency times as a function of the stirring rate, and, the theoretical profile of the metastable zone width as a function of the stirring rate (Mullin, 2001), as it can be seen in Figure 7.

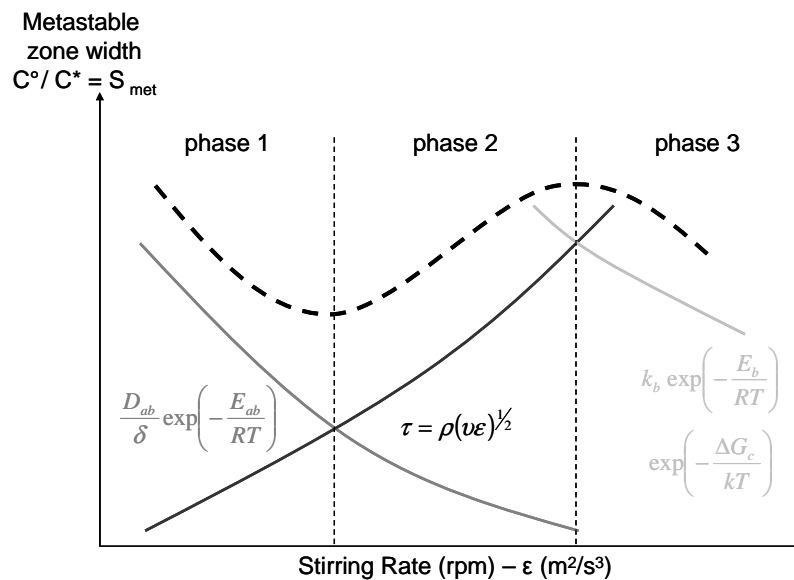


Figure 7: theoretical profile of the metastable zone width as a function of the mixing operating conditions (Mullin, 2001)

Three phases can be observed on this last profile. To understand the interpretation presented below, it is firstly important to remind that the increase of the stirring rate leads to an increase of the velocity gradients at different scales in the fluid, and, therefore to an increase of the turbulent kinetic energy dissipation rate  $\varepsilon$  [eq. (1)]:

$$\varepsilon = \frac{\nu}{2} \overline{\left( \frac{\partial u_i}{\partial x_j} + \frac{\partial u_j}{\partial x_i} \right)^2} \quad (1)$$

***Phase 1: decrease of the metastable zone width with increasing rotation speed.***

The turbulent kinetic energy of the flow is dissipated through heat in the Kolmogorov micro – swirl (smallest vortices of the turbulence) by the viscosity. The increase of the local temperature of the solution allows the crossing of molecular diffusion energy barrier,  $E_{ab}$ . Therefore, it leads to an increase of the solute diffusion coefficient,  $D$  [eq. (2)].

$$D = \frac{D_{ab}}{\delta} \exp\left(-\frac{E_{ab}}{RT}\right) \quad (2)$$

Moreover the increase of the mixing leads to the decrease of the diffusion boundary layer,  $\delta$ , and then to the increase of  $D$  [eq. (2)].

Those two phenomena account for the noticed decrease of the metastable zone width with increasing rotation speeds. Indeed, an increase of the diffusion kinetics  $D$  leads to an increase of the nucleation rate  $B$  [eq. (6)] (influence on the nucleation rate pre exponential coefficient  $K$ ).

***Phase 2: increase of the metastable zone width with increasing rotation speed.***

The increase of the turbulent kinetic energy dissipation rate also leads to the increase of the turbulent shear stresses,  $\tau$ . If the crystal size is smaller than the Kolmogorov micro - swirl size, the turbulent shear stresses are expressed as in eq. (3).

$$\tau = \rho(\nu\varepsilon)^{1/2} \quad (3)$$

These shear stresses remain negligible in phase 1 but become significant when the stirring rate increases, thus accounting for the noticed increase of the metastable zone width (Sherwood & Ristic, 2001).

***Phase 3: decrease of the metastable zone width with increasing rotation speed.***

While previous effects are still present in phase 3, two additional phenomena become significant. Indeed, the effect of the increased temperature, due to the increased turbulent kinetic energy dissipation rate, has a significant influence on two kinetics [eq. (4) & (5)]:

- the kinetics of incorporation of molecules in a nucleus :  $k_b \exp\left(-\frac{E_b}{RT}\right)$  (4)

- the kinetics of critical nucleus formation:  $\exp\left(-\frac{\Delta G_c}{kT}\right)$  (5)



## Crystallization of a polymorphic drug in a stirred tank

All these phenomena are in competition and lead to the form of the curve presenting the evolution of the metastable zone width as a function of the stirring rate [Figure 7]. (Mullin, 2001)

These qualitative concepts used to interpret the theoretical profile of the metastable zone width as a function of the stirring rate allow explaining the experimental profiles and the relative positions of the three curves in Figure 6.

For this purpose, some additional theoretical considerations must be taken into account regarding the nucleation rate.

It can be experimentally shown that the metastability curve for the morph I lies above the solubility and metastability curves of the morph II, at any stirring rate, during the crystallization process. Then, as it can be seen in Figure 1 (right), at the saturation concentration for the morph II at the maturation temperature (“point B” or “point C”), the system is characterized by a point located in the metastable zone of the morph I. In this zone, the nucleation rate,  $B(S(t))$  [eq. (6)], of the morph I is not spontaneous and is therefore quite slow.

$$B(S(t)) = K \exp\left(-\frac{E}{RT}\right) \exp\left(-\frac{16\pi}{3} \frac{\gamma^3 M_m^2}{k(\rho_s)^2 R^2 T^3 \ln^2(S(t))}\right) \quad (6)$$

In Figure 8, the rate of nucleation is schematically presented as a function of the relative sursaturation  $S$ , defined as the ratio between the concentration in the solution and the solubility at the same temperature ( $S = C / C^*$ ). The two curves correspond to two different stirring rates.

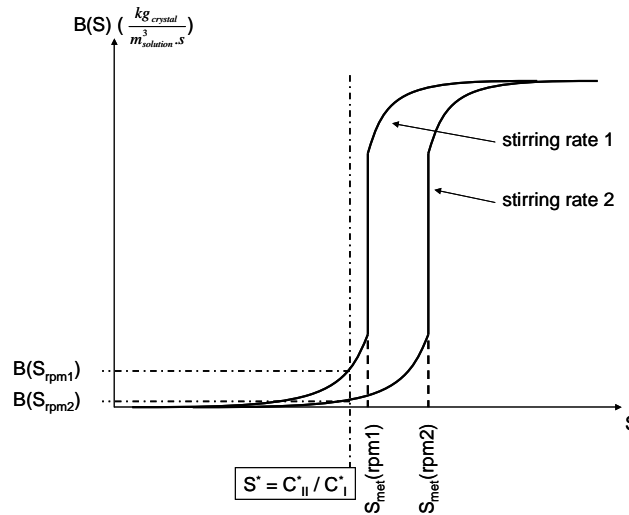


Figure 8: nucleation rate ( $B$ ) as a function of the relative sursaturation ( $S$ ) at two different stirring rates

Below the relative sursaturation characterising the metastability curve,  $S_{\text{met}} = C^{\circ} / C^*_I$ , the rate of nucleation is quite small.

Remembering that the nucleation of the morph I is the step which controls the beginning of the polymorphic transition, the latency time depends on the time needed to induce the nucleation.

As it can be seen in *Figure 8*, as the relative supersaturation characterizing the system before the polymorphic transition ( $S^* = C_{II}^* / C_I^*$ ) is fixed, the smaller the metastable zone width, the larger the nucleation rate, and the smaller the latency time.

Coming back to the experimental results of the latency times as a function of the stirring rate presented in *Figure 6*, a qualitative interpretation of the relative positions of the three curves can now be done. The curve relative to the anchor corresponds to the phase 1: the turbulent shear stresses are not important enough to allow the beginning of the phase 2. The curves which correspond to the propeller and the Rushton turbine are similar. Their relative position can be explained by the larger turbulent shear stresses in the fluid when the Rushton turbine is used. This leads to an earlier and more important increase for the curve presenting the latency times relative to the Rushton turbine than for the curve relative to the propeller.

#### 4. Discussion and Conclusions

The analysis of the results obtained by the optical microscopy, the in – situ FBRM probe and the on – line ammeter allow to affirm that the mechanism of polymorphic transition involves the nucleation of the morph I, the dissolution of the morph II and the growth of the morph I. The step which limits the beginning of the polymorphic transition is the morph I nucleation. This can also be concluded by the comparison between the experimental profiles of the latency times as a function of the stirring rate, and, the theoretical profile of the metastable zone width as a function of the stirring rate.

Up to now, the experimental results demonstrate, as it could be expected, the importance of the mixing operating conditions on the polymorphic crystallization process. We intend to investigate hydrodynamic local parameters of the fluid (Escudé R. et al., 2004), for various impellers types and stirring rates. These local parameters – turbulent kinetic energy dissipation rate, turbulent shear stresses at the Kolmogorov scale, ... – will be obtained by Computational Fluid Dynamics (Gambit & Fluent). The purpose of those future investigations is to build a universal correlation between experimental latency times and some hydrodynamic local parameters of the fluid.

#### Nomenclature

B nucleation rate  $\left( \frac{kg_{crystal}}{m^3_{solution} \cdot s} \right)$

C concentration  $\left( \frac{kg_{product}}{kg_{solution}} \right)$

$C^{\circ}_{I,II}$  concentration of the metastability curve relative to the morph I,II  $\left( \frac{kg_{product}}{kg_{solution}} \right)$

Crystallization of a polymorphic drug in a stirred tank

$C_{I,II}^*$	saturation concentration (of the solubility curve) of the morph I,II ( $\frac{kg_{product}}{kg_{solution}}$ )
D	solute diffusion coefficient ( $\frac{m}{s}$ )
$D_{ab}$	molecular diffusion coefficient ( $\frac{m^2}{s}$ )
$\delta$	diffusion boundary layer ( $m$ )
$\varepsilon$	turbulent kinetic energy dissipation rate ( $\frac{m^2}{s^3}$ )
E	activation energy of nucleation ( $\frac{J}{mol}$ )
$E_{ab}$	activation energy relative to the molecular diffusion ( $\frac{J}{mol}$ )
$E_b$	activation energy relative to the incorporation of molecules in a nucleus ( $\frac{J}{mol}$ )
$G_c$	activation energy relative to the formation of a critical size nucleus ( $J$ )
$\gamma$	surface tension ( $\frac{N}{m}$ )
k	Boltzmann constant ( $\frac{J}{K}$ )
$k_b$	kinetic coefficient of incorporation of molecules in a nucleus ( $\frac{m}{s}$ )
K	nucleation rate pre exponential coefficient ( $\frac{kg_{crystal}}{m^3_{solution} \cdot s}$ )
$M_m$	molar mass ( $\frac{kg}{mol}$ )
$\nu$	cinematic viscosity coefficient ( $\frac{m^2}{s}$ )
P	power dissipated in the solution ( $W$ )
R	perfect gas constant ( $\frac{J}{mol \cdot K}$ )
$\rho$	fluid density ( $\frac{kg}{m^3}$ )
$\rho_s$	solid density ( $\frac{kg}{m^3}$ )
S	relative sursaturation: $C / C^*$ (/)
$S^*$	relative sursaturation at the system initial state before transition: $C_{II}^* / C_I^*$ (/)

$S_{\text{met}}$	relative supersaturation at the metastability point: $C^{\circ} / C^{*}$ (/)
t	time (s)
T	temperature ( $^{\circ}\text{C} / \text{K}$ )
u	velocity ( $\frac{m}{s}$ )
x	spatial co – ordinate (m)

## References

- Baldyga J., Bourne J.R & Hearn S.J (1997) Interaction between chemical reactions and mixing on various scales, *Chemical Engineering Sciences*, 52:4, 547-466
- Barata P.A & Serrano M.L. (1996) Salting-out precipitation of potassium dihydrogen phosphate: II. Influence of the agitation intensity, *Journal of Crystal Growth*, 163, 426-433
- Escudié R., Bouyer D. & Liné A. (2004) Characterization of trailing vortices generated by a rushton turbine, *AIChE Journal*, 50, 75-86
- Garcia E., Hoff C. & Veessler S. (2002) Dissolution and phase transition of pharmaceutical compounds, *Journal of Crystal Growth*, 237-239, 2233-2239
- Garcia E., Veessler S., Boistelle R. & Hoff C. (1999) Crystallization and dissolution of pharmaceutical compounds: An experimental approach – *Journal of Crystal Growth*, 198/199, 1360-1364
- Kundu P.K & Cohen I.M. (2002) *Fluid Mechanics*, USA
- Mersmann A. (1995) *Crystallization Technology Handbook*, New York
- Mullin (2001) *Crystallization*, London
- Pohorecki R. & Baldyga J. (1983) The use of a new model of micromixing for determination of crystal size in precipitation, *Chemical Engineering Science*, 38, 79-83
- Sarkar D., Rohani S. & Jutan A. (2006) Multi-objective optimization of seeded batch crystallization processes, *Chemical Engineering Sciences*, 61, 5282-5295
- Sherwood J.N. & Ristic R.I (2001) The influence of the mechanical stress on the growth and dissolution of crystals, *Chemical Engineering Science*, 56, 2267-2280
- Veessler S., Puel F. & Fevotte G. (2003) Polymorphism in process of crystallization in solution, *STP PHARMA PRATIQUES*, 13, n°2 May / June

## Acknowledgments

The authors wish to thank UCB – Pharma Company, based in Braine l'Alleud – Belgium for their financial and technical support of this research. C. Herman acknowledges financial support from the ARC (Action de Recherches Concertées), Belgium.